07 - 10 September 2009

PROCEEDINGS

54. IWK

Internationales Wissenschaftliches Kolloquium
International Scientific Colloquium

Information Technology and Electrical Engineering - Devices and Systems, Materials and Technologies for the Future

Faculty of Electrical Engineering and Information Technology

Startseite / Index:
http://www.db-thueringen.de/servlets/DocumentServlet?id=14089

TECHNISCHE UNIVERSITÄT
ILMENAU

Impressum

Herausgeber: Der Rektor der Technischen Universität Ilmenau
Univ.-Prof. Dr. rer. nat. habil. Dr. h. c. Prof. h. c.
Peter Scharff

Redaktion: Referat Marketing
Andrea Schneider

Fakultät für Elektrotechnik und Informationstechnik
Univ.-Prof. Dr.-Ing. Frank Berger

Redaktionsschluss: 17. August 2009

Technische Realisierung (USB-Flash-Ausgabe):
Institut für Medientechnik an der TU Ilmenau
Dipl.-Ing. Christian Weigel
Dipl.-Ing. Helge Drumm

Technische Realisierung (Online-Ausgabe):
Universitätsbibliothek Ilmenau
ilmedia
Postfach 10 05 65
98684 Ilmenau

Verlag:
Verlag ISLE, Betriebsstätte des ISLE e.V.
Werner-von-Siemens-Str. 16
98693 Ilmenau

ISBN (USB-Flash-Ausgabe): 978-3-938843-45-1
ISBN (Druckausgabe der Kurzfassungen): 978-3-938843-44-4

Startseite / Index:
http://www.db-thueringen.de/servlets/DocumentServlet?id=14089

SYNTHESIS AND CHARACTERIZATION OF TI-DOPED BARIUM HEXAFERRITE POWDERS BY GLASS CRYSTALLIZATION TECHNIQUE

Pamela Quiroz, Bernd Halbedel

Ilmenau University of Technology, Institute of Material Engineering
Department of Inorganic – Nonmetallic Materials

ABSTRACT

Barium hexaferrite ($BaFe_{12}O_{19}$) has attracted much attention for microwave device applications because of its large uniaxial magnetocrystalline anisotropy, high resistivity and permeability at high frequencies [1].
The chemical substitutions of iron by titanium show that it strongly affects the magnetic properties and improve the microwave properties.
Such modified barium hexaferrite powders were obtained following the glass crystallization technique (GCT) using the basic composition (mole-%): 40 BaO + 33 B_2O_3 + (27-x) Fe_2O_3 + x TiO_2, with different melt doping rates of TiO_2 [2].
For the characterizations of the powders chemical analyses, X-ray diffraction, SEM, vibration sample magnetometer and measurement of the microwave heating were used to obtain their structure and their magnetic properties.

Index Terms **–** Ferrite, crystallization, cation substitution, magnetic properties**.**

1. INTRODUCTION

The regular barium hexaferrite (BHF) has the crystal structure of the mineral magnetoplumbite (see Figure 1).

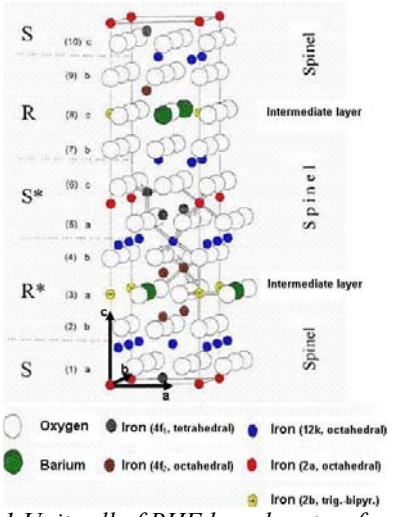

Figure 1 Unit cell of BHF based on two formula of $BaFe_{12}O_{19}$ [3]

It belongs to the group of hexagonal ferrite of the so-called M-type. The crystallographic unit cell contains two molecules of the chemical composition $BaFe_{12}O_{19}$.

Within the basic structure the Fe^{3+} ions occupy five different interstitial sites. Three sites named 12k, 2a and $4f_2$ have an octahedral coordination, one site $4f_1$ has a tetrahedral coordination and the 2b site has a five-fold coordination with the oxygen ions. The number in the expression of the different sites indicates the number of Fe^{3+} ions per unit cell [3-5].

The magnetic moments of the iron ions are aligned collinear to the hexagonal c-axis. The ordering of the magnetic moments of the ferric ions and the strong
superexchange interaction over the oxygen ions explains the excellent magnetic behavior of this material. Opposite spin directions cause a ferrimagnetic structure [3, 5].

It is known that Fe ions provide the largest positive contribution at the 2*b* site, a relative weak positive contribution at the 12*k* and 2*a* sites, and a negative contribution at the $4f_1$ and $4f_2$. In Table 1 are summarized the crystallographic and magnetic properties of the five lattice sites of barium hexaferrite.

Lattice site	Coordination	Number of Fe^{3+} - Ion	Spin direction
12k	octahedral	6	up
$4f_1$	tetrahedral	2	down
$4f_2$	octahedral	2	down
2a	octahedral	1	up
2b	trig.-bipyramidal	1	up

Table 1 Spin directions for the Fe^{+3} cation sublattices of M-type barium hexaferrite [6]

Hence the substitutions of other ions for Fe ions could lead to changes of the magnetic structure and magnetic properties.

M-type doped BHF has been intensively studied; the idea of doping the BHF is to improve the magnetic properties, in order to change the magnetocrystalline anisotropy. There is a possible a wide range of cation substitutions in BHF according to Kojima [7]. Ti - doped BHF $BaFe_{12-x}Ti_xO_{19}$ obtained using the conventional ceramic method was investigated in [8] and [9].

In [8] it is estimated according to neutron and X-ray diffraction experiments that at low concentrations the Ti^{4+} ions ($x \leq 0.2$) occupy preferentially the octahedral $4f_2$ sites of the magnetoplumbite structure. Simultaneously with the Ti^{4+} substitution an equivalent amount of Fe^{3+} ions has to be converted into Fe^{2+} ions, which are probably situated as nearest neighbors in the same sublattice as the Ti^{4+} ions are located in the $4f_2$ sites. The result of this substitution is an increase of the c-lattice parameter, in spite of the smaller Ti^{4+} radius compared with Fe^{3+}. Also higher magnetic anisotropy constants K_1 were measured. However with larger doping rates K_1 decreased again. That applies also to the saturation magnetization M_S. That contradicts the expectations. If the Ti^{4+} ions are located on the $4f_2$ sites, then M_S must increase, because the magnetic moment of the Ti^{4+} ions is zero and the spin direction of the lattice site $4f_2$ is down. The Ti^{4+} ions are also installed on other lattice sites (with spin-up directions) or the collinear magnetic structure is disordered due to the change of the exchange interactions to the immediate neighbours.

According to the results in [9] the magnetic properties (M_S, K_1) of the doped samples ($x \leq 2$) are smaller than the values of undoped BHF samples. This behavior attributed to the superposition of two independent factors: the limitation of the collinear adjustment of the magnetic moments aligned along the preferred magnetic crystallographic easy axes, and the unequal replacement of Fe^{3+} by Ti^{4+} ions in the octahedral (75%) and tetrahedral sites (17%).

In this work, we are looking for the possible Ti^{4+} ion substitutions in BHF by the glass crystallization technique to change the magnetic properties ($_JH_c$ and M_S) of BHF and study the dependences of the properties on the substitution rate.

Applications of Ti^{4+} doped BHF powders are micro wave absorbing materials in order to

- reduce the electromagnetic radiation exposure on biological systems or
- assure the safe operation of instruments and equipments as well as the security (prevention of wireless signal leakages) or
- facilitate the modern applications fundamentally and/ or with larger efficiency.

2. EXPERIMENTAL PROCUDURE

The doped flakes were synthesized according to the GCT using the basic composition 40 mole-% BaO + 33 mole-% B_2O_3 + (27-x) mole-% Fe_2O_3 +xTiO_2. The different melt dopings were x= 1.8, 3.6, 5.4, 7.2 and 9.0 mole-% TiO_2 and the respective flakes were named according to the Table 2.

The flakes Ti0_01 correspond to the undoped BHF and were used as a reference to analyze the effect of the grade of substitution.

Probe	Melt doping mole-% TiO_2
Ti0_01	0
Ti1_01	1.8
Ti3_01	3.6
Ti5_01	5.4
Ti7_01	7.2
T19_01	9

Table 2 Name of flakes according to the melt dopings

GCT is a technique for preparing submicron to nanoscaled particles of doped barium hexaferrite and this involves

- the synthesis of an intermediate glassy phase in the ternary phase system Fe_2O_3-BaO-B_2O_3,
- the crystallization of the ferrite particles from the amorphous phase as well as
- the separation of the ferrite particles from the glass phase.

Figure 2 shows a schematic representation of the GCT. [9]

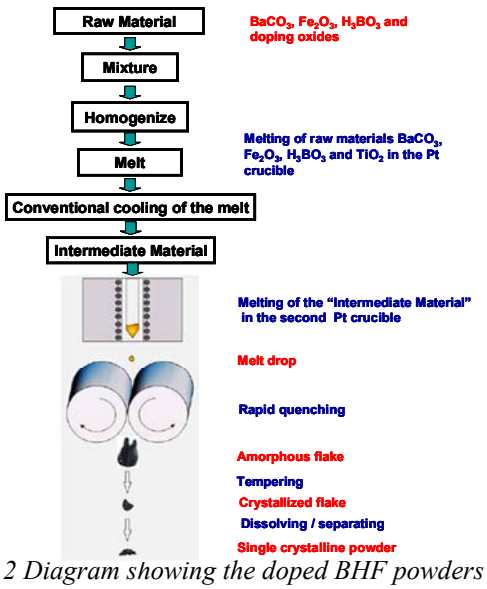

Figure 2 Diagram showing the doped BHF powders preparation process using GCT

The raw materials $BaCO_3$, Fe_2O_3, H_3BO_3 and TiO_2 were dried for 24 h at 100°C before weighing them, and then they were mixed and homogenized.
A Pt crucible was filled with the raw materials; it was introduced inside an electric furnace at 1350°C for 2 hours.
After 2 hours the primary melt was cooled over the cold plate at 8°C for 15 minutes to obtain the primary melt.
The primary melt was powdered and sifted up to a size of 125 µm and in this way the "intermediate material" was obtained.
This material was melt again in the Pt-crucible with an outlet nozzle at 1350°C using a rapid quenching machine.

The droplets are quenched between two rotating steel rollers with a surface temperature of 8°C and a speed of 130 min^{-1} and thus cooled down rapidly. In this way amorphous flakes were formed with a thickness of approx. (75 – 100) µm, a length of approx. 70 µm and a width of approx. 45µm.

In order to obtain the barium hexaferrite powders it was necessary to anneal the flakes in a furnace at a temperature higher than the glass transformation temperature but below the melting [1].

The necessary annealing temperature was determinated by Differential Scanning Calorimetry (DSC). In addition the samples were powdered so that the particle sizes were < 63 µm.

The used process parameters for the crystallization are shown in the next Table:

Flakes	melt doping	Process conditions				Powder
	TiO_2 [mole-%]	melting	Crystallization			
			Heating rate	Temperature	Time	
Ti0_01	0	2 h at 1350 °C	>> (infinite)	840°C	2h	Ti0b_01
Ti1_01	1.8			840°C		Ti1b_01
Ti3_01	3.6			840°C		Ti3b_01
Ti5_01	5.4			840°C		Ti5b_01
	5.4			680°C		Ti5c_01
	5.4			800°C		Ti5d_01
Ti7_01	7.2			840°C		Ti7b_01
Ti9_01	9			840°C		Ti9b_01

Table 3 Temper conditions

Samples of 10 g were tempered under the conditions described in Table 3. The heating rate was quite high, since the samples were placed from room temperature directly into a pre-heated furnace, was the same for all the samples, as well as the tempering time period (2 hours) and the tempering temperature (840°C).

For the case of flakes Ti5_01 two additional tempering temperatures (680°C and 800°C) were used to analyze its particular crystallization behavior.

After tempering, the material must be powdered and sifted (< 63µm) again.

The purpose was to get a particle size suitable for the acid treatment process in order to dissolve completely the borate glass matrix. Each sample was treated with 100 ml of acetic acid (20% CH_3COOH) and heated for 30 min at 97°C.

The ferrite particles were separated from the solution with a magnet; these was carefully rinsed and centrifuged at 7500 min^{-1}, and finally dried at 120°C. In this way the dispersed monocristalline BHF powders were obtained.

3. RESULTS AND DISCUSSION

In Figure 3 the DSC - signals for undoped and different doped flakes in dependence on the temperature are shown.

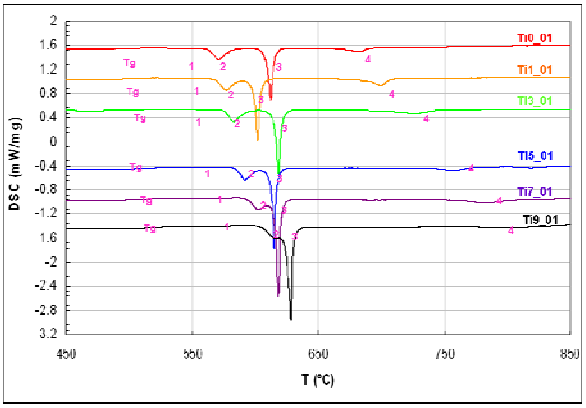

Figure 3 Comparison of the DSC - signals for undoped and different doped flakes at the heating rate of 5K/min in air in dependence on the temperature

We can clearly observe in the DSC curves for each doped flake four exothermic peaks at different temperatures and the Glass Transition Temperature (T_g). The temperature values for the 4 peaks and T_g obtained for each sample are shown in Table 4; these values change according to the amount of dopant.

Sample	DSC					TG [wt-%]
	T_g	Peak 1	Peak 2	Peak 3	Peak 4	mass change
Ti0_01	485.3°C	556.0°C	563.0°C	608.8°C	665.2°C	0.12
Ti1_01	485.1°C	558.8°C	569.2°C	598.8°C	683.5°C	0.12
Ti3_01	492.1°C	557.3°C	575.7°C	615.5°C	698.3°C	0.11
Ti5_01	496.9°C	560.5°C	584.5°C	612.7°C	687.8°C	0.08
Ti7_01	502.6°C	561.1°C	593.8°C	616.1°C	759.6°C	0.08
Ti9_01	502.3°C	569.8°C	604.6°C	624.7°C	771.1°C	0.07

Table 4 Temperature values of the peaks of the DSC curves and mass change of TG curves for undoped and doped BHF

The Ti0_01 (undoped flakes) is used as a control for observing the crystallization behavior when increasing the melt doping of Ti.

We can observe in Table 4, that the T_g values hardly change for small melt dopings (< 5.4 mole-% TiO_2), but T_g, increases with increasing melt dopings. Apparently the Ti substitutions slightly modify this characteristic point and it is located around 494.0 ± 7.9 K.
Further the results show a consistent increase in the temperature value for peaks 2 and 4 with increasing melt doping, whereas peak 3 presents an incoherent behavior at increasing melt dopings.

The crystallization of flakes without and with other dopings (e.g. Co^{2+}/Ti^{4+}, Mn^{2+}/Ti^{4+}) is widely investigated with simultaneous studies of DSC, XRD and TEM to analyze the phases formed during the annealing. [10-12]

From these investigations the ***first peak*** does not correspond to formation of new phases (no new peaks in the corresponding XRD diagram), it represents the oxidation of Fe^{2+} to Fe^{3+}.
The ***second peak*** results from the precipitation of an iron-rich phase not yet clearly identifiable with a particle size of about D ~ 5nm.
The ***third peak*** corresponds to the precipitation of BaB_2O_4 and the early stages of the crystallization of barium hexaferritic particles at nanometric level, with D ~ 20 nm.
The ***fourth peak*** corresponds to the further growth of BHF crystals, D ~ 50 nm. These crystals have a hexagonal bipyramidal morphology within a BaB_2O_4 matrix.

At temperatures higher than the fourth peak, the typical hexagonal plates, characteristic for BHF, are obtained. The BHF particles sizes are in the range 50 nm up to 500 nm depend on the dopings (type and rate).

In the Figure 4 TG analyzes for all samples are shown, the behavior of the mass increase with increasing temperature can be seen. A mass increase is observed between 300 and 600 ºC.

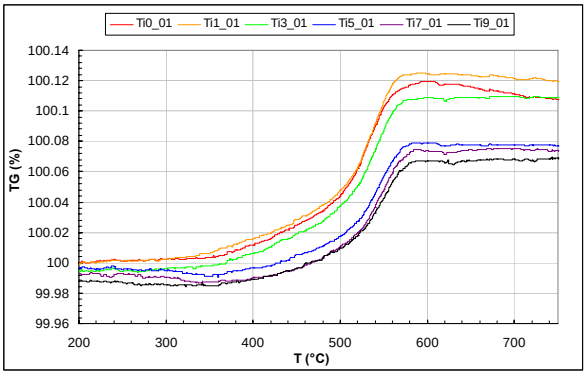

Figure 4 TG-curves for undoped and different doped flakes in dependence on the temperature at heating rate of 5 K/min in air

It results from an oxidation by oxygen absorption from air and diffusion into the flakes. The Fe^{2+} ions contained in the flakes oxidize to Fe^{3+} [12].

Here, a lower increase of mass is observed with increasing melt doping x ≥ 5.4 mole-%. The corresponding mass change values are shown in Table 4.

For the case of flakes Ti5_01, new exothermic peaks appeared in the DSC diagram at about 710°C and 825°C. Therefore these flakes were investigated at tempering temperatures 680°C and 800°C in order to analyze the phases of this doped material [2].

The X-ray diffraction diagrams of all the powders are show in Figure 5.

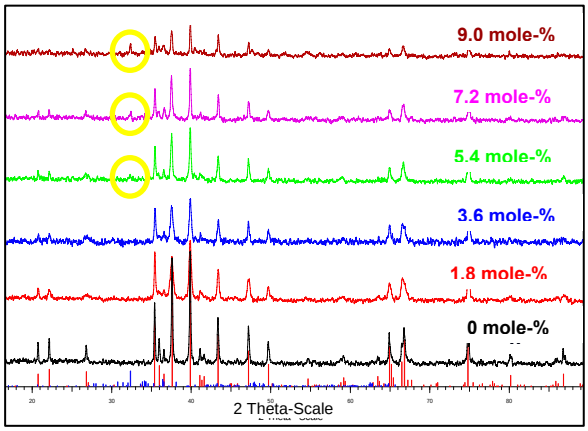

Figure 5 Comparison of the XRD-diagrams for undoped and Ti-doped BHF powders

X-ray diffraction measurements confirm that the Ti0b_01, Ti1b_01 and Ti3b_01 powder samples are single phase. The diffraction patterns correspond to the Card Nº 43-0002 for undoped BHF which proves that the crystal structure remains essentially unchanged. However, there is a significant difference in the relative intensities of the peaks; the relative intensities of the peaks decrease when the melt doping concentrations increase. This is possibly due to a deformation of the host lattice and the decreasing of the crystal sizes (see Figure 10). Starting from melt dopings ≥ 5.4 mole-% (Ti5b_01, Ti7b_1 and Ti9b_01) small peak at 2θ= 32.4° related to $BaTi_6O_{13}$ can be observed. This reveals the formation of a new phase and corresponds with the DSC analyses in Figure 3.

Analyzing the effect of the tempering temperature, we can observe in Figure 6 that for the Ti5c_01 sample at a tempering temperature of 800°C, the peak at 2θ= 32.4° is not observed; the diffraction lines for this sample correspond to the BHF pattern. There are no extra lines, which leads to believe that a single phase is only formed under these conditions.

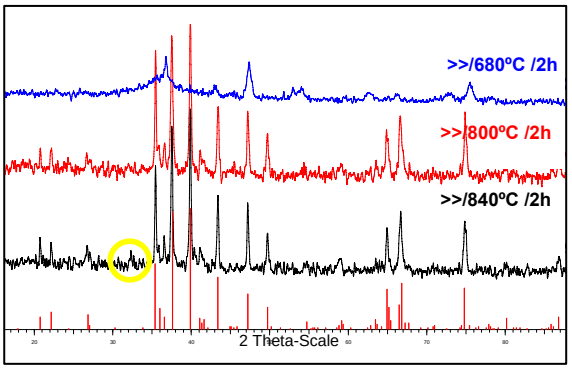

Figure 6 Comparison of the XRD-diagrams for Ti-doped BHF powders Ti5b,c,d - Effect of the tempering temperature.

For Ti5d_01, X-ray diffraction shows that there is not a complete crystallization. This temperature is not sufficiently to receive the full formed crystalline structure of BHF.
Thus it is clear that this new phase observed for x ≥ 5.4 mole-% in the Figure 5, forms at higher temperatures (here: at 840 ° C).

Figure 7 shows that most of the Ti ions get into inside the ferrite phase during the crystallization. From the amounts of raw materials we calculated the theoretical substitution ratio in the power ("x" in BHF formula) and from the ICP results these values are also obtained.

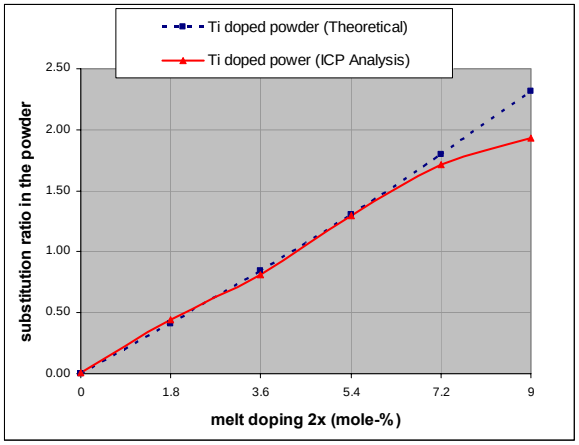

Figure 7 Cation substitutions in dependence on melt doping for BHF

The broken line in Figure 7 shows the expected theoretical behavior and the red line the real behavior. For melt dopings < 5.4 mole-% the values are approx. identically. However, if the increasing of the melt doping continues the linearity is lost because the new phase $BaTi_6O_{13}$ is formed. The difference is largest in the Ti9b_01 sample. Powder dopings to x ≈ 2 are obtained.

Density measurements at the powders confirm the partial substitution of iron ions by titanium ions.

In the following figure we can observe the change of density in dependent on the substitution rate x.

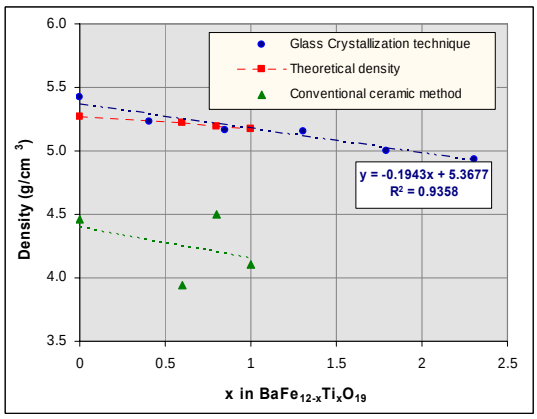

Figure 8 Density of Ti doped BHF powders in dependent on the substitution rate x and comparison of the density obtained by conventional ceramic method [8]

The powder density decreases linear when the substitution rate increases. This is understandable because the atomic mass of Ti^{4+} is smaller than the Fe^{3+}.
Also Figure 8 shows a comparison between the variation of density for the Ti doped BHF obtained by means of GCT and the conventional ceramic method. The densities obtained by GCT are closer to the theoretical densities than those obtained by the conventional ceramic method in [8].

The SEM micrographs of the synthesized powders are shown in Figure 9.
It is to be noticed that the particles of all samples exhibit a plate-like, nearly hexagonal shape. The samples obtained at the same tempering conditions show acceptable quality of the crystallization.

A variation in the melt doping concentrations alters the size of the BHF platelets. This is understandable, because the radius of Fe^{3+} (0.67 Å) is larger than that of Ti^{4+} (0.61 Å).
In addition the melt doping influences the nucleation und the crystal growth. This behavior is shown in the Figure 10.

The diagonal (a^*_{50}) of the platelets varied between 50 and 270 nm. The crystal sizes of undoped BHF powders are largest and then a^*_{50} decreases with rising melting doping and after a^*_{50} increases again.

Assumedly, first the melt doping of the barium borate melts with TiO_2 promotes the nucleation of BHF, so that at the same annealing conditions the number of nucleus increases with the melt doping, however its growth is limited due to the existing quantities. That leads to smaller crystal sizes. At higher doping concentrations (> 5.4 mole-% TiO_2) a^*_{50} increases due to the formation of further phases ($BaTi_6O_{13}$, see Figure 5).

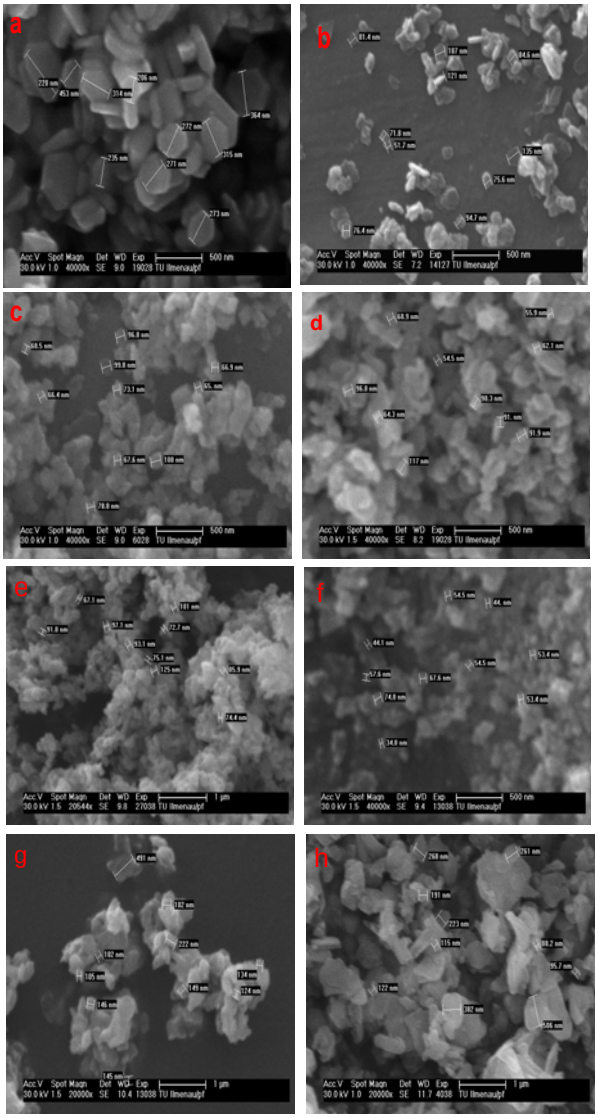

Figure 9 SEM micrographs for BHF powders with different doping concentrations
a) Ti0b_01(0 mole-%), b) Ti1b_01(1.8 mole-%), c) Ti3b_01(3.6 mole-%), d) Ti5b_01(5.4 mole-%), e) Ti5c_01(5.4 mole-%), f) Ti5d_01(5.4 mole-%), g) Ti7b_01(7.2 mole-%), h)Ti9b_01(9.0 mole%)

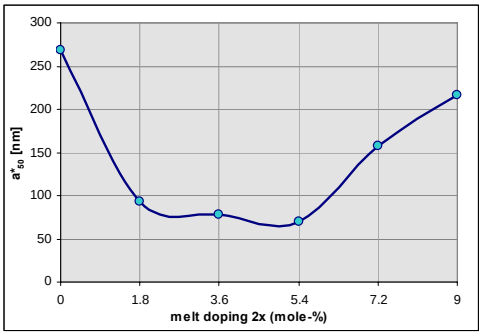

Figure 10 Dependencies of a^*_{50} for the Ti-doped BHF powders by variation of melt doping concentration

The interest in this work was to study a possible influence of Ti ions substitution in decreasing the anisotropy. This would be reflected in a lower $_JH_C$ and a higher saturation M_S when the Ti^{4+} ions occupied the $4f_2$ sites in the structure of BHF.

We observed in Table 5 that a small substitution of Ti does not have a pronounced effect on static magnetic properties, larger concentrations have the desired effect on the $_JH_C$ but M_S also decreased, this should not happen if the Ti^{4+} ions occupy only the positions $4f_2$, so that we can assume these ions occupy other positions in the lattice of BHF.

Sample	x_{th}	Tempering conditions	M_S [kA/m]	$_JH_c$ [kA/m]	$M_S/_JH_c$	Density
Ti0b_01	0	<< / 840°C / 2h / <<	171.9	360.5	0.48	5.424 ± 0.062
Ti1b_01	0.27	<< / 840°C / 2h / <<	72.7	295.1	0.25	5.233 ± 0.016
Ti3b_01	0.81	<< / 840°C / 2h / <<	76.8	320.4	0.24	5.167 ± 0.024
Ti5b_01	1.3	<< / 840°C / 2h / <<	90.84	229.97	0.40	5.151 ± 0.024
Ti5c_01	*1.3*	*<< / 800°C / 2h / <<*	*74.13*	*187.2*	*0.40*	*5.055 ± 0.007*
Ti5d_01	*1.3*	*<< / 680°C / 2h / <<*	*2.63*	*57.24*	*0.05*	*5.109 ± 0.010*
Ti7b_01	1.71	<< / 840°C / 2h / <<	58.16	136.5	0.43	4.999 ± 0.020
Ti9b_01	1.93	<< / 840°C / 2h / <<	48.12	89.54	0.54	4.936 ± 0.009

Table 5 Magnetic properties, density and crystallization conditions of Ti-doped BHF powders

Figure 11 shows the dependences of $_JH_C$ and M_S with the melt doping concentration at same tempering conditions (see full line curves).

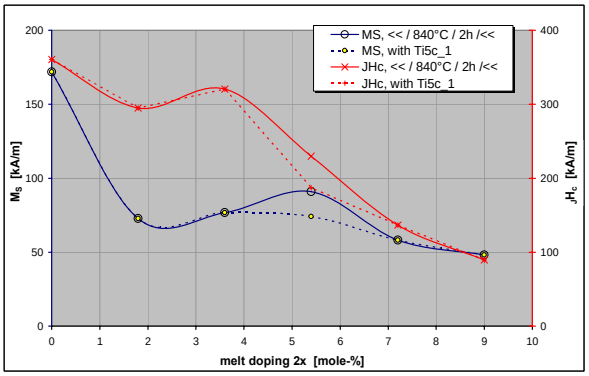

Figure 11 Dependencies of coercitivity and saturation magnetization for Ti-doped BHF powders by variation of melt doping concentration

An irregular variation in the static magnetic properties can be recognized with increasing melt dopings 2x. However, the tendency shows that the magnetic properties of the original hard magnetic behavior of BHF powders can be shifted to soft magnetic behavior, also with Ti- dopings. But, a new phase develops for melt dopings ≥ 5.4 mole-% TiO_2. Without change the crystallographic structure (M-type) succeeds only if one anneals the sample Ti5_01 with 800 °C. Then the $_JH_c$ continues to decrease, however the saturation magnetization decrease likewise (see broken lines in Figure 11).

The behavior of these magnetic properties are not similar to others doped BHF powders e.g. Co^{2+}/Ti^{4+}, Mn^{2+}/Ti^{4+} [15]. At only Ti^{4+} doped BHF powders the

M_S remains almost constant with small melt dopings, but the $_jH_c$ decreases too slowly and a new phase develops. That can affect with controlled crystallization. The detailed investigation of the crystallization behavior of TiO_2 doped rich iron barium borate melts will be a topic of the research in the future.

For the quantitative characterization of the microwave absorption the heating curves ΔT(t) of the powders are determined in a special prepared microwave oven at 2,45 GHz with an IR sensor (see Figure 12).

The powders were pressed in a quartz crucible. The powder mass and compression is equal for all measurements, so that the heating curves can be compared directly [16].

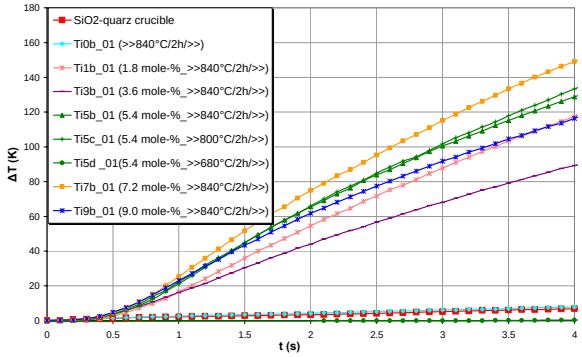

Figure 12 ΔT-t Diagram of the BHF containing different amounts of dopants

As we can observe in Figure 12, the heating curve of the Ti7b_01 sample exhibits the highest temperature values. This powder absorbs best die microwave radiation. In contrast to it the temperature increase of the quartz crucible and also the powder Ti0b_01 is negligibly small. Both not absorb microwave energy.

Not a lot of difference exists in absorption among the samples Ti5b_01 and Ti5c_01, however in Ti5d_01 the absorption is null, here the crystallization temperature is much lower than the previous ones and therefore the phase formation is insufficient (see Figure 6).

Figure 13 shows the relation between the different melt dopings (x = 1.8, 3.6, 5.4, 7.2 and 9.0 mole -% TiO_2) and the calculated heating rate ΔT/Δt corresponding to the registered temperature within the range from 1 to 2 s.

This diagram confirms that the powder Ti7b_1 exhibits the best absorptive capacity and the dependence on the doping is nonlinear. Also for this detailed investigations are necessary in the future.

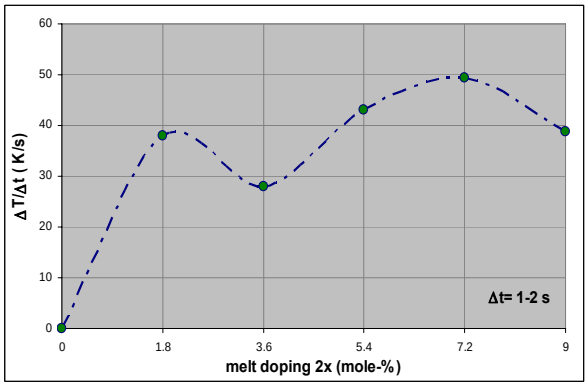

Figure13 Heating rate ΔT/Δt depending on the melt doping 2x (mole-%)

4. CONCLUSIONS

Concerning synthesis procedures of the Ti doped BHF, GCT allows to control both: particle size and morphology. We obtained powders with different particle sizes and a platelet-like shape. Powders dopings up to x ≈ 2 were obtained. With the installation of the Titatium ions in BHF a certain part remains bivalent iron ions. In resuming work the assumption of the valence stability should be confirmed with XPS (X-ray Photoelectron Spectroscopy) measurements.

By XRD it was demonstrated that a new phase develops in the samples Ti5b_01, Ti7b_01 and Ti9b_01, which corresponds to $BaTi_6O_{13}$. This phase can be eliminated if the flakes are annealed at smaller temperatures. But the crystallization behavior in dependence of the temperature must be known. In addition further investigations are necessary.

The results of this study show that the magnetic properties depend on the melt doping rate. However, this behavior is not similar to others doped BHF powders e.g. Co^{2+}/Ti^{4+}, Mn^{2+}/Ti^{4+} [15].
At low concentrations of Ti^{4+}, the $_jH_C$ is not influenced, but with high concentrations the $_jH_C$ decreases as it is know. The M_S decreased when increases concentrations of Ti^{4+}. Thus also with the glass crystallization technique the Ti^{4+} ions do not only occupy the position $4f_2$, otherwise the saturation magnetizations M_S would have to increase.
The powders should also be analyzed by Mössbauer spectroscopy and neutron diffraction to determine the location of all the ions in the lattice. It is possible that with a progressive Ti substitution, the Ti^{4+} ion occupies other type of sites, for example places like 12k, 2b or 2a.

According to M_S and $_jH_C$ measurements, the substitution of Fe^{3+} by Ti^{4+} is related to the observed improvement of the dielectric properties at microwave

frequencies of barium hexaferrites, so that it is possible to use this ferrite as a microwave absorber. That proven with measurements of the heating curves ΔT(t) in a special prepared microwave oven at 2,45 GHz. Ti7b_1 exhibits the best absorptive capacity. The heating rate in the microwave field amounts approx. 50 K/s.

5. ANKNOWLEDGMENT

I would like to acknowledge the "Pontificia Universidad Católica del Perú" and the institute of Material Engineering at the Ilmenau University of Technology for the opportunity to participate in the academic interchange program and the DAAD for the funding. Thanks to this I can make this work.

6. REFERENCES

[1] B. Halbedel, D. Hülsenberg, St. Belau, U. Schadewald, M. Jakob, Synthese und Anwendungen von maßgeschneiderten $BaFe_{12-2x}A^{II}_xB^{IV}_xO_{19}$-Pulvern. cfi/Ber. DKG 82, No. 13, S. 182-188, 2005.

[2] P. Quiroz, Investigation of the synthesis of single crystalline, Ti-doped barium hexaferrite powders by glasscrystallization technique. Master thesis, Pontificia Universidad Catòlica del Peru, Lima, 2008.

[3] B. Halbedel, S. Belau, M. Jakob, D. Hülsenberg, F. Niemz, T. Schulze, M. Mooz, G. Carl, Novel Ferrimagnetic Fibers and Fleeces for Innovative Aplications. 7th International Symposium „Alternative Cellulose" Rudolstadt, 06. – 07. September 2006.

[4] S. Rösler, P. Wartewig, H. Langbein, Synthesis and characterization of hexagonal ferrites $BaFe_{12-2x}Zn_xTi_xO_{19}$ ($0 \leq x \leq 2$) by thermal decomposition of freeze-dried precursors. Cryst. Res. Technol. Vol. 38, Nº 11, 927-934, 2003.

[5] P. Wartewig, M.K. Krause, P. Esquinazi, S. Roslerb, R. Sonntag, Magnetic properties of Zn- and Ti-substituted barium hexaferrite. Journal of Magnetism and Magnetic Materials 192 (1999) 83-99.

[6] B. Halbedel, K. Müller, Magnetische Eigenschaften von Bariumhexaferritpulvern und daraus hergestellter Formkörper, ALCERU-HighTech Workshop, TU Ilmenau, 22.09.2005.

[7] H. Kojima, Ferromagnetic materials, Vol. 3. E. P. Wohlfarth (Ed.), North Holland, Amsterdam, 1982.

[8] P. A. Mariño-Castellanos, J. Anglada-Rivera, A. Cruz-Fuentes, R. Lora-Serrano, Magnetic and microstructural properties of the Ti^{4+}-doped Barium hexaferrite. Journal of Magnetism and Magnetic Materials 280 (2004) 214-220.

[9] V.A.M. Brabers, A.A.E. Stevens, J.H.J. Dalderop, Z. Simga, Magnetization and magnetic anisotropy of $BaFe_{12-x}Ti_xO_{19}$ Hexaferrites, Journal of Magnetism and Magnetic Materials 196-197 (1999) 312-314.

[10] D. Hülsenberg, O. Knauf, B. Hamann, Glass Crystallization Technique for ultrafine ceramic powders. DKG 71 Nº 11-12, 707-711, 1994.

[11] B. T. Shirk, W. R. Buessem, Magnetic Properties of Barium Ferrite Formed by Crystallization of a Glass. Journal of The American Ceramic Society, Vol. 53, Nº 4, 192-196, 1970.

[12] U. Schadewald, B. Halbedel, H. Romanus, D. Hülsenberg, New Results of the Crystallization Behavior of Hexagonal Barium Ferrites from a Glassy Matrix. Mat.-wiss. u. Werkstofftech. 2006 37 No. 11.

[13] M. El-Hilo, H. Pfeiffer, Magnetic properties of barium hexaferrite powders, Journal of Magnetism and Magnetic, 129 (1994), 339-347, 1994.

[14] C. Doppleb, R. Lipfert, Herstellung magnetischer Strukturen auf der Basis von Bariumhexaferrit. 43th International Scientific Colloquium, TU Ilmenau, 1998.

[15] B. Halbedel, S. Belau, Synthesis of Partial Mn^{2+}/Ti^{4+}-Substituted Single Crystalline Barium Hexaferrite Powders by Glass Crystallization Technique. ECERS 2007, June 17-21, Berlin 10th International Conference and Exhibition of the European Ceramic Society.

[16] B. Halbedel, M.K. Güzelarslan, M.K, Erarbeitung eines optimierten Verfahrens zum Aufbereiten von Spezialpigment-Slurrys und anschließendem Beschichten von Papier zum Zwecke elektromagnetischer Abschirmung im Hochfrequenzbereich. Schlussbericht, IGF-Vorhaben Nr. 200 ZGB, 01.02.2006 – 31.04.2008.

Authors:

MSc. Quiroz, Pamela
Dr.-Ing. Halbedel, Bernd
Ilmenau University of Technology,
Institute of Material Engineering
Department of Inorganic – Nonmetallic Materials
Gustav-Kirchhoff-Straße 6
D-98683 Ilmenau/ Germany

Corrosponding author:
Phone: +49 (0) 3677 69 2487
Fax: +49 (0) 3677 69 1436
E-mail: bernd.halbedel@tu-ilmenau.de